ARTICLE

Bariatric Surgery

Secretin release after Roux-en-Y gastric bypass reveals a population of glucose-sensitive S cells in distal small intestine

Ida M. Modvig [1,2] · Daniel B. Andersen[1,2] · Kaare V. Grunddal[1] · Rune E. Kuhre[1,2] · Christoffer Martinussen[3] ·
Charlotte B. Christiansen[1,2] · Cathrine Ørskov[1] · Pierre Larraufie[4] · Richard G. Kay[4] · Frank Reimann [4] ·
Fiona M. Gribble[4] · Bolette Hartmann[1,2] · Kirstine N. Bojsen-Møller[3] · Sten Madsbad[3] ·
Nicolai J. Wewer Albrechtsen[1,5,6] · Jens J. Holst [1,2]

Abstract
Objectives Gastrointestinal hormones contribute to the beneficial effects of Roux-en-Y gastric bypass surgery (RYGB) on glycemic control. Secretin is secreted from duodenal S cells in response to low luminal pH, but it is unknown whether its secretion is altered after RYGB and if secretin contributes to the postoperative improvement in glycemic control. We hypothesized that secretin secretion increases after RYGB as a result of the diversion of nutrients to more distal parts of the small intestine, and thereby affects islet hormone release.
Methods A specific secretin radioimmunoassay was developed, evaluated biochemically, and used to quantify plasma concentrations of secretin in 13 obese individuals before, 1 week after, and 3 months after RYGB. Distribution of secretin and its receptor was assessed by RNA sequencing, mass-spectrometry and in situ hybridization in human and rat tissues. Isolated, perfused rat intestine and pancreas were used to explore the molecular mechanism underlying glucose-induced secretin secretion and to study direct effects of secretin on glucagon, insulin, and somatostatin secretion. Secretin was administered alone or in combination with GLP-1 to non-sedated rats to evaluate effects on glucose regulation.
Results Plasma postprandial secretin was more than doubled in humans after RYGB ($P < 0.001$). The distal small intestine harbored secretin expressing cells in both rats and humans. Glucose increased the secretion of secretin in a sodium-glucose cotransporter dependent manner when administered to the distal part but not into the proximal part of the rat small intestine. Secretin stimulated somatostatin secretion (fold change: 1.59, $P < 0.05$) from the perfused rat pancreas but affected neither insulin ($P = 0.2$) nor glucagon ($P = 0.97$) secretion. When administered to rats in vivo, insulin secretion was attenuated and glucagon secretion increased ($P = 0.04$), while blood glucose peak time was delayed (from 15 to 45 min) and gastric emptying time prolonged ($P = 0.004$).
Conclusions Glucose-sensing secretin cells located in the distal part of the small intestine may contribute to increased plasma concentrations observed after RYGB. The metabolic role of the distal S cells warrants further studies.

✉ Nicolai J. Wewer Albrechtsen
hgk795@ku.dk

✉ Jens J. Holst
jjholst@sund.ku.dk

Extended author information available on the last page of the article

Introduction

In the duodenum, enteroendocrine S cells secrete secretin in response to luminal acidification and thereby regulate the intraluminal milieu by stimulating the exocrine pancreas to secrete water and bicarbonate [1]. Secretin, however, also has other actions including the inhibition of gastric emptying [2–4] and has been suggested to regulate the secretion of the pancreatic islet hormones [5–10].

Gastrointestinal hormones, including glucagon-like peptide-1 (GLP-1), are currently used for the treatment of metabolic diseases and endogenous GLP-1 contributes to the glucose lowering and weight reducing effect of

Roux-en-Y gastric bypass (RYGB) [11, 12]. Whereas it is well established that GLP-1 secretion is increased after RYGB in humans [13], it is unknown if secretin secretion is increased.

Glucose is a powerful stimulus for GLP-1 secretion [14] and is rapidly absorbed in the upper part of the small intestine, therefore intraluminal concentrations are low in the distal part of the small intestine. We hypothesized that the delivery of glucose to the distal small intestine, as seen after the diversion following RYGB, stimulates secretin secretion by luminal-sensing mechanisms. To address this, we measured plasma secretin before and after RYGB. Furthermore, we isolated and perfused the upper or lower half of the rat small intestine and studied the effect of intraluminal glucose on secretin secretion as well as the molecular sensors involved.

To investigate the potential effects of secretin on blood glucose and secretion of islet hormones, we administered secretin subcutaneously to conscious rats and perfused, in separate experiments, the rat pancreas, testing the effects of secretin on glucagon, insulin, and somatostatin secretion.

Materials and methods

Ethical approvals

Human studies: Written informed consent was obtained from all study participants, and the study was approved by the Municipal Ethics Committee of Copenhagen in accordance with the Helsinki-II declaration and by the Danish Data Protection Agency, and registered at www.clinicaltrials.gov (NCT01993511).

Animal Studies: Animal studies were conducted with permission from the Danish Animal Experiments Inspectorate, Ministry of Environment and Food of Denmark, permit 2018-15-0201-01397, and in accordance with the EU Directive 2010/63/EU and guidelines of Danish legislation governing animal experimentation (1987), the National Institutes of Health (publication number 85-23), and approved by the local ethical committee (EMED, P18-336).

Peptides

GLP-1 7–36NH$_2$, rat and human secretin were obtained from Bachem (cat no. 4030663, cat no. 4037181 and cat no. 4031250, Bubendorf, Switzerland). Radioactive labeled rat and human secretin was obtained from Phoenix Pharmaceuticals, Inc (cat no. T-067–06 and T-067-07, CA, USA). Development and evaluation of a secretion radioimmunoassay are described in Supplementary Materials 1.

Mixed-meal tests before and after RYGB surgery in obese subjects

Plasma obtained during a standardized liquid mixed-meal test before, 1 week, and 3 months after RYGB from 13 obese subjects (type 2 diabetes; $n = 4$, impaired glucose tolerance; $n = 3$, normal glucose tolerance; $n = 6$) was analyzed. Glucose tolerance was determined by standard OGTT preoperatively. All samples were from a study by Martinussen et al. as previously described [15].

Distribution of secretin and GLP-1 along the gastrointestinal tract in humans and rats

Mass-spectrometry based detection was used to assess the distribution of secretin and GLP-1 (for comparison) in human intestinal tissue as described previously [16]. The secretin and GLP-1 profiles are presented as peak area divided by tissue weight.

Whole-wall tissue biopsies (~1 cm) of esophagus, ventricle, duodenum, proximal jejunum, distal ileum, and colon were collected from non-fasted rats (anatomical definitions are listed in Supplementary Table 1). Peptides in tissue biopsies were extracted using trifluoroacetic acid (Supplementary Materials 2), and immunohistochemical staining of secretin-positive cells was performed on paraffin embedded tissue samples using anti-secretin (5585–3), a generous gift from Professor Jan Fahrenkrug (Supplementary Materials 3).

Animal experiments

Male Wistar rats (200–250 g) were obtained from Janvier (Le Genest-Saint-Isle, France) and housed two to four rats per cage. Rats were allowed 1 week of acclimatization and kept on a 12 h light/dark cycle with ad libitum access to water and standard chow.

Isolated perfused rat small intestine and pancreas

Perfusion was performed using a single pass perfusion system (UP100, Hugo Sachs Harvard Apparatus, Germany). The rat small intestine and pancreas were surgically isolated (as described in Supplementary Materials 4). Each protocol started with a baseline period followed by the addition of various test substances. Test stimulants used in the perfused intestine included 0.1 M HCl, 0.1 M NaHCO$_3$$^-$, 0.05 M KCl (Sigma-Aldrich, Brøndby, Denmark), 20% (w/v) D-glucose (cat no. G8270, Sigma-Aldrich, Denmark), and 10 mmol/L Phloridzin (cat no. P3449, Sigma-Aldrich, Denmark). Test stimulants used in the perfused pancreas were 1 nmol/L GLP-1 7–36NH$_2$ and both 20 pmol/L and 2 nmol/L secretin.

In vivo experiments in rats

Experiments were carried out on two occasions on fasted rats (300 ± 13 g) just before their nocturnal feeding period (5:00 PM). Rats were divided into weight-matched groups ($n = 8$/group). At -10 min, $200\,\mu\text{L}$ tail blood was collected into prechilled EDTA-coated capillary tubes (catalog no. 200 K3E, Microvette; Sarstedt, Nümbrecht, Germany) and instantly transferred onto ice. At -5 min, $300\,\mu\text{L}$ test solution was injected subcutaneously. Test solutions were isotonic saline, (negative control) or peptides prepared in isotonic saline: secretin (30 nmol/kg), GLP-1 (30 nmol/kg) or secretin + GLP-1 (both 30 nmol/kg). At 0 min, a bolus of D-glucose (2 g/kg) and acetaminophen (100 mg/kg), prepared in isotonic saline, was given orally. Rats from the same cage received different treatments. Blood was collected at times -10, -5, 5, 15, 30, 45, 60, and 90-min. Glucose was measured immediately after blood collection, while the remainder of the samples were instantly transferred onto ice and centrifuged ($1650 \times g$, 4 °C, 10 min) within half an hour to obtain plasma. Plasma was transferred to Eppendorf tubes, immediately frozen on dry ice and stored at -20 °C until analysis.

Biochemical measurements of perfusion effluents, rat blood and rat plasma

Perfusion effluents: insulin was measured with antiserum (code no. 2006–3) which cross-reacts with rodent insulin I and II [17]. Glucagon was measured with an antibody directed against the C-terminus (code no. 4305) as previously described [18]. Total GLP-1 (the sum of $7\text{–}36\text{NH}_2$, $9\text{–}36\text{NH}_2$ and potential mid-terminal cleaved fragments) was measured using a C-terminal specific radioimmunoassay targeting amidated forms (code no. 89390) [19]. Somatostatin was measured using a side-viewing antibody (code no. 1758–5), detecting all the bioactive forms of somatostatin [20, 21].

Blood glucose was measured using a glucometer (Accu-Chek Mobile, catalog no. 05874149001; Roche Diagnostics, Mannheim, Germany). Plasma concentrations of glucagon were measured by sandwich ELISA (catalog no. 10-1281-01; Mercodia AB, Uppsala, Sweden) [22]. Plasma concentrations of insulin and C-peptide were measured using ELISAs (catalog no. 10-1250-01 and 10-1172-01; Mercodia AB, Uppsala, Sweden).

RNA sequencing of human islets

Publicly available RNA-seq dataset (from GSE85241, GSE81608 and E-MTAB-5061 [23–25]) were obtained. Average reads per kilobase million values for secretin

receptor (Sctr) and GLP-1 receptor were uploaded to the Jupyter Notebook (http://jupyter.org/). Data were then $\log_2$ transformed and mean expression levels were calculated in alpha, beta, and delta cells, respectively. We excluded individuals with diabetes from these analyses. For further details about the donors, isolation of cells, and RNA-sequencing methods please see the original studies [23–25].

In situ hybridization on rat pancreases is described in Supplementary Materials 5.

Statistical analysis

Clinical samples and in vivo data: plasma concentrations of hormones were evaluated using area under the curve analysis and statistical testing by one-way ANOVA followed by Holm–Sidak multiple comparisons test. A mixed-effect model was applied in order to test the effect of treatment and time on the variables.

Perfusion experiments: data are expressed as mean ± SEM concentrations in venous effluents (pmol/L). Since the perfusion flow was kept constant through the experiments, this mirrors the actual secretion output (which can be calculated by multiplying with the flow rate). To test for statistical significance, mean values within the test period (based on 10 subsequent minutes) were compared with mean values in the baseline period (10 subsequent minutes prior to test stimulant administration) using statistical testing as described above.

Calculations were made using STAT14 (SE), College Station, Texas, USA. For illustrations, GraphPad Prism version 8.0 (GraphPad Software, La Jolla California USA) and Adobe CC software suite were used (San Francisco, CA, USA). P values < 0.05 were considered statistically significant. Data are shown as means ± SEM.

Results

Development of a sensitive secretin assay

We generated titer curves for three different antibodies against human secretin (structure in Fig. 1a) using two radioactive iodine-labeled secretin peptides (termed tracer). Based on binding characteristics, the antibody named 5595–3 was selected for further testing and for the preparation of calibrator curves (Supplementary Fig. 1). By sequencing alignment, we found that human and rat secretin differ at position 14–16 (human: REG vs. rat: QDS) (Fig. 1a) but no species variation was found within the antibody's epitope (position 18–27) (Fig. 1a). For rat samples, we therefore used the same antibody and tracer. For calibrating purposes, we included the rat isoform of secretin as calibrator control.
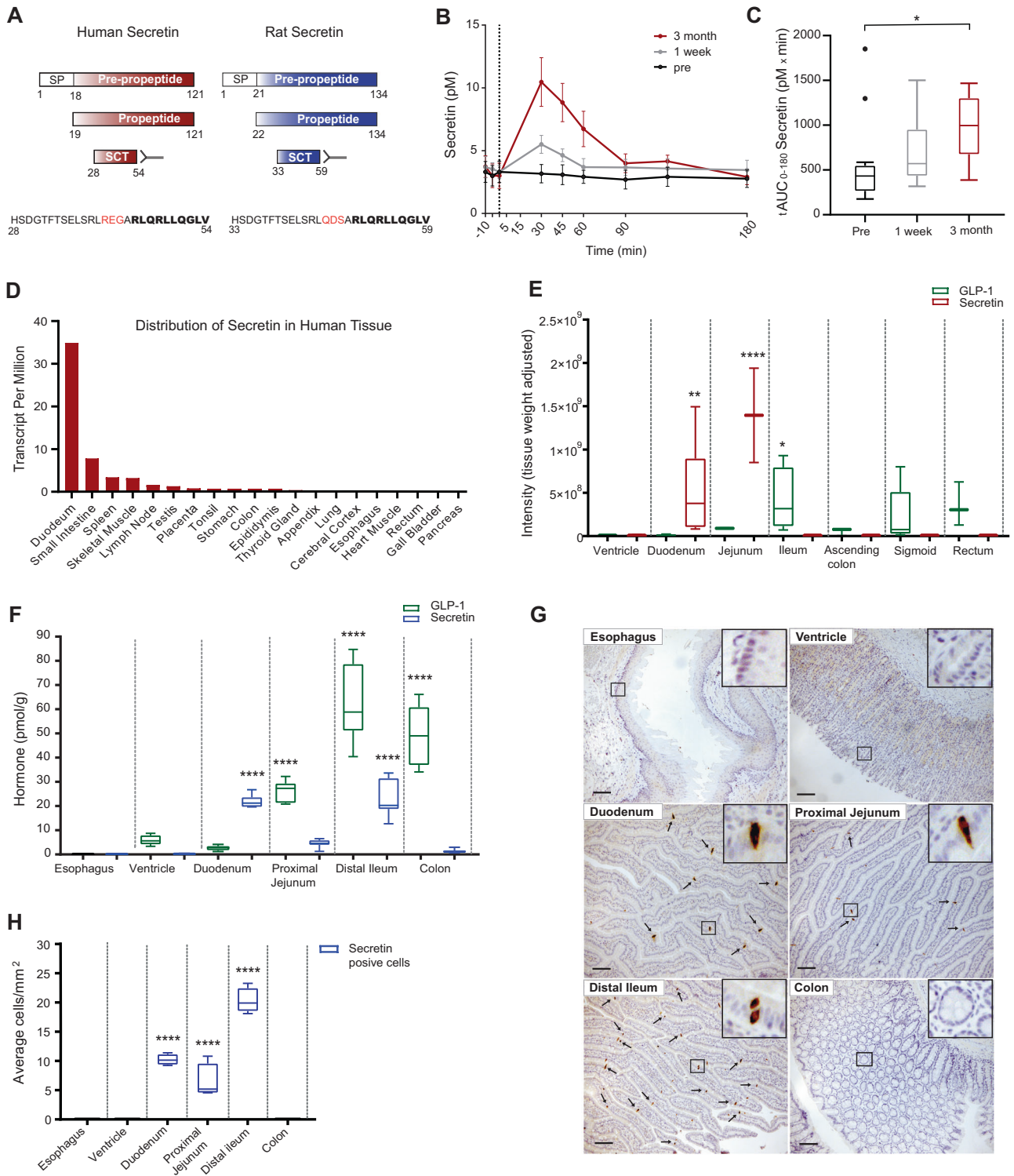
Recovery of human secretin added to human pooled plasma was calculated to $71 \pm 11\%$ (mean ± SD) with a lower limit of detection of 1 pmol/L and a dynamic range from 2.5 to 80 pmol/L (Supplementary Fig. 1) using solvent phase-extraction (70% ethanol). We did not observe cross-reactivity (not significantly different compared with background) toward CCK, glucagon, glicentin, GLP-1, human insulin, oxyntomodulin, neurotensin, and PYY at concentrations up to 300 pmol/L.

Comparison of commercial ELISAs

The two commercially available ELISAs had low recoveries of human secretin of $15 \pm 8\%$ (mean ± SD) in assay

Fig. 1 Secretion of secretin after Roux-en Y gastric bypass surgery and distribution of secretin in rats and in humans. a Structure of human and rat secretin and antibody binding in the secretin assay. SP signal peptide. Red capitals: differences between rat and human peptide sequences. Highlighted capitals: Ab epitope. **b** Postprandial plasma concentrations of secretin before (pre), 1 week, and 3 months after RYGB surgery in obese individuals, $n = 13$. **c** Calculated total area under the curve (tAUC0-180) is shown for panel **b**. **d** Expression profiles of secretin in human tissues. RNA-seq data from human tissues presented as transcripts per million (TPM) [26]. **e** Distribution of secretin and GLP-1 in human intestinal tissue. Mass-spectrometry profiling of secretin and GLP-1 in the human gastrointestinal tract. Levels of secretin and GLP-1 are presented as peak area divided by tissue weight, $n = 2–9$ [16]. **f** Extractable secretin and GLP-1 concentrations in whole-wall biopsies along the rat gastrointestinal tract (pmol/g tissue), $n = 7$ male Wistar rats. **g** Immunohistochemical staining of secretin in the rat gastrointestinal tract (Ab:5585–3, 1:20.000), $n = 4$ male Wistar rats. **h** Counting of secretin-positive cells (immunohistochemistry) along the rat gastrointestinal tract (cells/mm²), scale bar 100 μm, $n = 4$ male Wistar rats. Data are shown as means ± SEM. $P > 0.05$. $*P < 0.05$, $**P < 0.01$, $****P < 0.0001$ by a one-way ANOVA with correction for multiple testing (Holm–Sidak).

buffer. A Bland–Altman analysis (comparing the concentrations measured using the two ELISAs to the in-house developed RIA) showed acceptable (<2 SD) degree of variation for concentrations above 20 pmol/L, however, for physiological plasma concentrations of secretin (<20 pmol/L) the two commercial ELISAs were inadequate (Supplementary Fig. 2).

Having developed a specific and sensitive secretin radioimmunoassay, we next investigated whether postprandial plasma secretin concentrations are elevated after RYGB surgery.

RYGB surgery increases meal-induced secretin release in obese individuals

Fasting plasma concentrations of secretin were not significantly different after comparison with before RYGB (Fig. 1b, $P > 0.45$), whereas postprandial plasma secretin concentrations in response to a liquid meal test were significantly increased 3 months after compared with before RYGB ($P < 0.05$), reaching a two- to threefold higher peak value, and total AUCs were approximately doubled (tAUC0–$_{18 min}$: 569 ± 475 vs. 956 ± 360 pmol/L × min) (Fig. 1c). Concentrations were also increased 1 week after RYGB but to a more modest degree and total AUCs did not differ from preoperative AUCs ($P = 0.67$).

Distribution of secretin in humans and rats

Using publicly available RNA-seq data from 37 different human tissues [26] expression profiles of secretin showed a maximum in the duodenum, as expected. However, high levels were also found in the more distal parts of the small

intestine (Fig. 1d), consistent with previous reports on secretin distribution in other species [27, 28]. Mass-spectrometry analysis on human gastrointestinal tissue revealed that secretin concentrations were highest in the duodenum as well as in jejunal biopsies (Fig. 1e). Concentrations of GLP-1 7–36NH₂ were included as positive controls. GLP-1 concentration was highest in the distal part of the gastrointestinal tract (ileum, colon, and rectum) (Fig. 1e) in line with previous reports [29].

To examine if the distribution of secretin in rats was similar to humans, we measured the concentration of extractable secretin from esophagus to colon in rats (Supplementary Table 1). Secretin was not detectable in esophagus and the ventricle (Fig. 1f, $n = 7$) but in the duodenum and in the distal ileum, secretin was found at comparable concentrations ~20–30 pmol/g tissue (Fig. 1f, $n = 7$). Concentrations of GLP-1 increased from duodenum to colon with the highest concentration in the distal ileum (~60 pmol/g tissue) (Fig. 1f, $n = 7$) in line with a previous report [30]. Immunohistochemical stainings of secretin (Fig. 1g, h) showed no staining in esophagus, ventricle, and colon and high intensity in proximal jejunum and distal ileum, consistent with the measured extractable concentrations.

Secretin responses from the proximal and distal small intestine using the isolated perfused rat intestine model

Luminal infusion of HCl increased secretin secretion fourfold (Baseline: 3.7 ± 0.9 vs. HCl: 15.6 ± 2.3 pmol/L, $P < 0.05$, $n = 6$) (Fig. 2a, b). Following HCl infusion, the intestine was flushed with sodium bicarbonate (0.1 M) to neutralize luminal pH (Fig. 2a). This returned secretin secretion to pre-HCl-stimulatory levels. KCl (0.05 M) was infused intravascularly at the end of the experiment (Fig. 2a). Secretion of secretin increased significantly compared with preceding baseline secretion (Baseline: 5.2 ± 0.8 vs. KCl: 9.1 ± 0.9 pmol/L, $P < 0.05$, $n = 6$) (Fig. 2b). Our data therefore suggests that cell depolarization is involved in secretin release from the perfused rat small intestine and furthermore that our perfusion model reflects the physiology of secretin secretion. We therefore decided to evaluate potential differences in HCl and glucose-induced secretin secretion in the proximal and distal small intestine using this model.

Differential sensing of glucose by secretin producing cells in the proximal and distal small intestine

Luminal HCl infusion increased secretin secretion ($P < 0.05$) from both the proximal and distal half of the small intestine, but to the greatest extent in the distal half
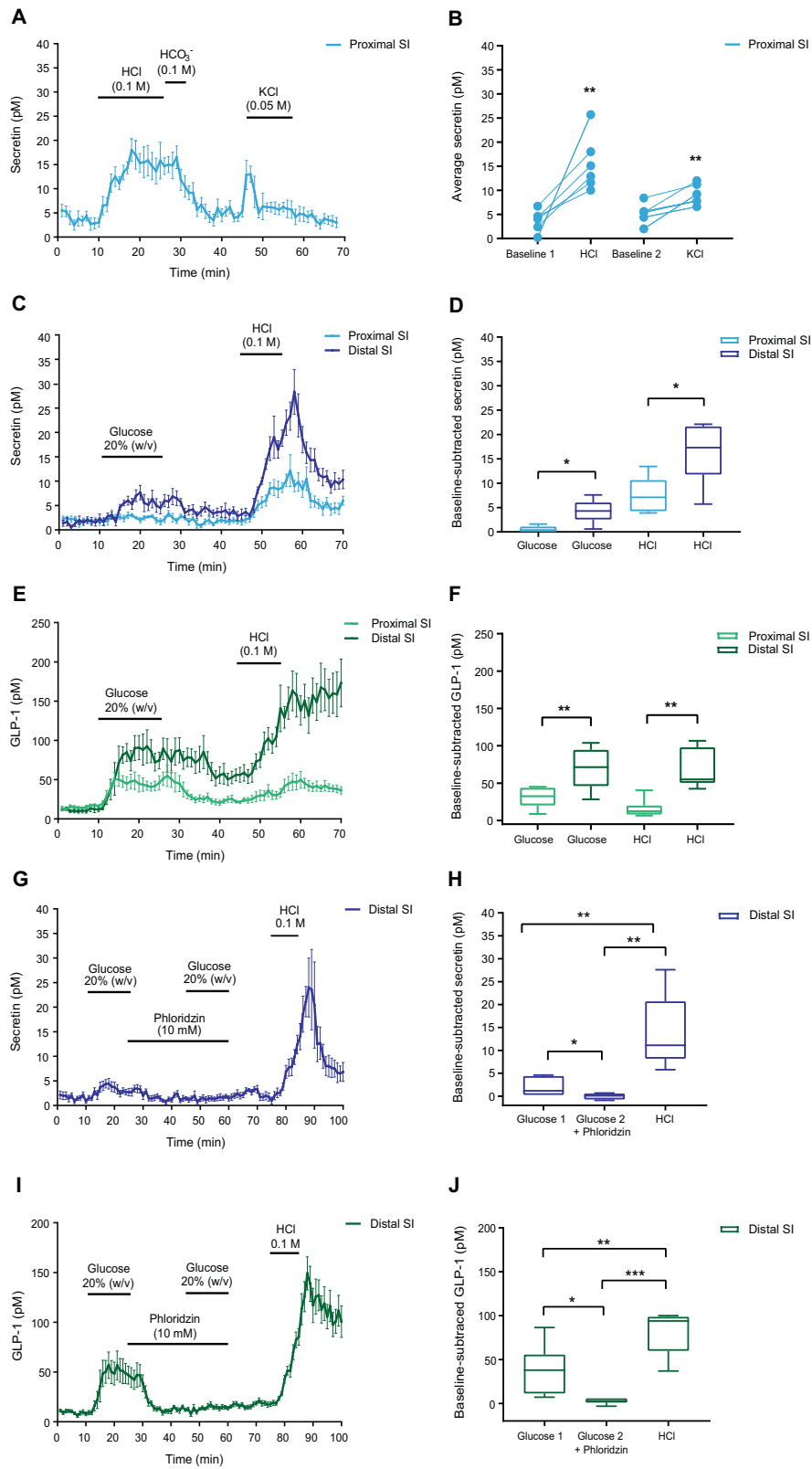
(baseline-subtracted values; Proximal. HCl: 7.6 ± 1.5 vs. Distal. HCl: 16.3 ± 2.6 pmol/L, P < 0.05, n = 6) (Fig. 2c, d). Of particular notice, distal, but not proximal, infusion

of glucose resulted in a significant (P < 0.05) secretin response (baseline-subtracted values; Proximal. Glucose: 0.48 ± 0.3 vs. Distal. Glucose: 4.3 ± 1 pmol/L, n = 6)

Fig. 2 Differential sensing of glucose by secretin-secreting cells in the perfused proximal vs. distal rat small intestine. a–b Validation of the perfused rat intestine as a model to study secretin release. HCl (0.1 M) was infused intraluminally between 11 and 25 min, $NaHCO_3^-$ (0.1 M) was infused between 26 and 30 min. KCl (0.05 M) was infused intravascularly between 46 and 60 min. **a** Secretin concentrations in venous effluents (pmol/L). **b** Mean concentrations of secretin at baseline (Baseline 1 and 2) and following stimulation with either luminal HCl or vascular KCl. **c–f** Differential sensing of glucose in the proximal vs. distal intestine. Glucose (20% w/v) was intraluminally infused between 11 and 25 min in either the proximal or the distal isolated perfused rat small intestine. HCl (0.1 M) was intraluminally infused between 46 and 55 min as a positive control for secretin release. **c** Secretin concentrations (pmol/L). **d** Mean baseline-subtracted secretin concentrations in response to glucose and HCl stimulation. **e** GLP-1 concentrations (pmol/L). **f** Mean baseline-subtracted GLP-1 concentrations in response to glucose and HCl stimulation. **g–j**: Sodium-coupled glucose transporters (SGLT) are involved in distal glucose sensing. Glucose (20% w/v) was infused intraluminally between 11 and 25 min and between 46 and 60 min. Phloridzin (10 mmol/L), an SGLT inhibitor, was infused intraluminally between 26 and 60 min. HCl (0.1 M) was infused intraluminally between 76 and 85 min as a positive control for secretin release. **g** Secretin concentrations (pmol/L). **h** Mean baseline-subtracted secretin concentrations in response to HCl and glucose stimulation with and without phloridzin. **i** GLP-1 concentrations (pmol/L). **j** Mean baseline-subtracted GLP-1 concentrations in response to HCl stimulation and glucose stimulation with and without phloridzin. Data are shown as means ± SEM. $P > 0.05$. $*P < 0.05$, $**P < 0.01$, $***P < 0.001$, by a one-way ANOVA with correction for multiple testing (Holm–Sidak), $n = 6$ male Wistar rats for all groups.


(Fig. 2c, d) suggesting that distally located secretin cells are capable of sensing glucose.

GLP-1 secretion was measured as this is a well validated control in this experimental setup [31, 32]. Secretion of GLP-1 in response to both glucose and HCl infusion was likewise significantly higher from the distal small intestine compared with the proximal small intestine (Fig. 2e, f), which is consistent with high extractable concentrations of GLP-1 in the distal small intestine (Fig. 1f).

Glucose-induced secretin secretion from the distal small intestine is mediated by sodium-glucose cotransporter

Inhibition of SGLT with the competitive SGLT1/2 inhibitor, phloridzin, eliminated glucose-stimulated secretin response from the distal rat small intestine (baseline-subtracted values; Glucose: 1.9 ± 0.7 vs. Glucose + Phloridzin: 0 ± 0.2 pmol/L, $P < 0.05$, $n = 6$) (Fig. 2g, h), indicating that sodium-coupled glucose absorption is involved in the mechanism of glucose-stimulated secretin secretion from the distal rat small intestine.

Consistent with previous reports [33, 34], phloridzin eliminated glucose-stimulated GLP-1 secretion from the distal rat small intestine (baseline-subtracted values;
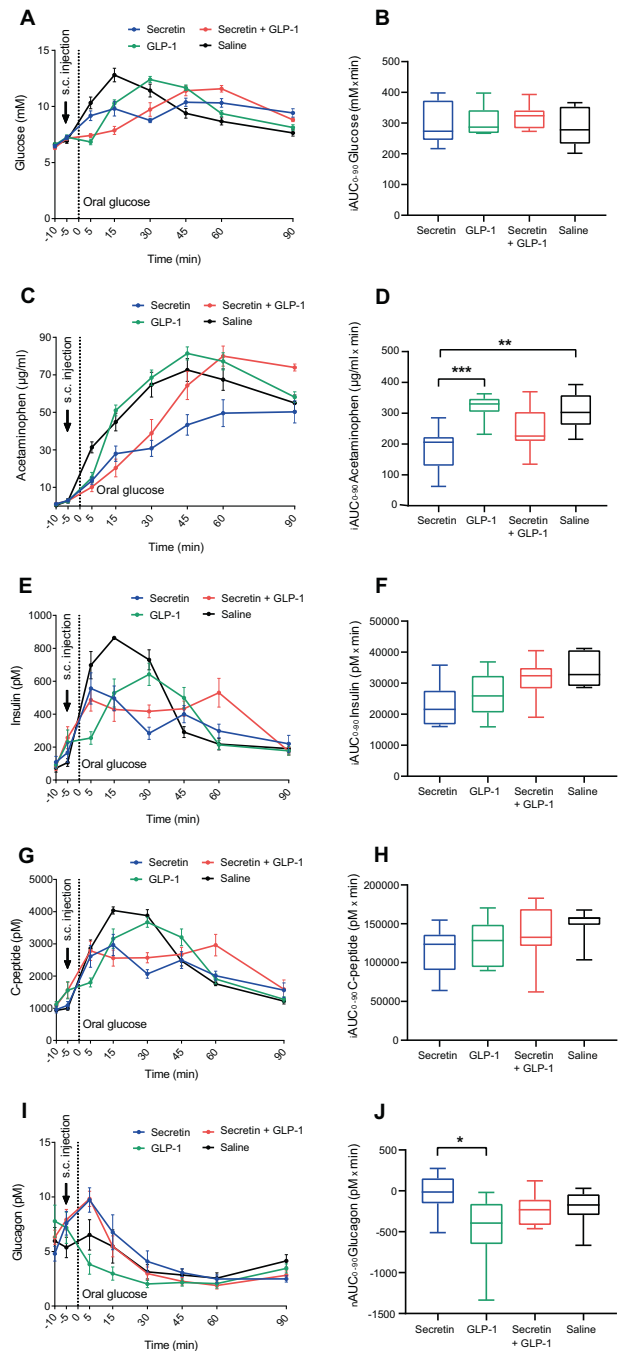
Glucose: 38.5 ± 10.4 vs. Glucose + Phloridzin: 2.6 ± 1.2 pmol/L, $P < 0.05$, $n = 6$) (Fig. 2i, j). HCl was included as a positive control for secretin secretion in the end of each experiment.

Secretin delays blood glucose peak time and increases plasma glucagon in non-sedated rats

Blood glucose concentrations were similar across groups at baseline ($P > 0.71$). Peak times for blood glucose were prolonged from 15 min (saline group) to 30 min (GLP-1),

Fig. 3 Effects of secretin and GLP-1 on glucose metabolism in non-sedated rats. Secretin (30 nmol/kg), GLP-1 (30 nmol/kg) or Secretin + GLP-1 (both 30 nmol/kg) were subcutaneously injected at timepoint -5 min. At timepoint 0, a mixture of oral glucose (2 g/kg) and acetaminophen (25 mg/mL) was given. **a** Blood glucose concentrations (mmol/L). **b** Incremental area under the curve ($iAUC_{0-90}$) of blood glucose concentrations shown in **a**. There were no significant differences in $iAUC_{0-90}$ between the groups ($P > 0.77$). **c** Plasma acetaminophen concentrations (μg/mL). **d** $iAUC_{0-90}$ of acetaminophen concentrations. Acetaminophen concentrations in the group receiving secretin were significantly decreased compared with the control group ($P < 0.05$) and to the group receiving GLP-1 ($P < 0.05$). **e** Plasma concentrations of insulin (pmol/L) **f** $iAUC_{0-90}$ of insulin concentrations. There were no significant differences in iAUC between the four groups ($P > 0.08$). **g** Plasma concentrations of C-peptide (pmol/L) **h** $iAUC_{0-90}$ of C-peptide concentrations. There were no significant differences between the groups ($P > 0.09$). **i** Plasma glucagon concentrations (pmol/L). **j** $iAUC_{0-90}$ of glucagon concentrations. Secretion of glucagon was significantly decreased in the group receiving GLP-1 compared with the group receiving secretin ($P < 0.05$). There were no significant differences between all other groups ($P > 0.32$). Data are shown as means ± SEM. $P > 0.05$. *$P < 0.05$, **$P < 0.01$, ***$P < 0.001$, by a one-way ANOVA with correction for multiple testing (Holm–Sidak). Data was also analyzed using a mixed-effect model to investigate statistical significance across time and treatment. $n = 31$ male Wistar rats (7–8 per group).

45 min (secretin), and 60 min (secretin + GLP-1) (Fig. 3a) but the incremental area under the curve ($iAUC_{0-90\,min}$) was not significantly different between groups ($P > 0.77$, Fig. 3b). Gastric emptying, reflected by changes in plasma acetaminophen concentrations, was markedly prolonged in secretin-treated rats compared with saline and GLP-1 treated groups ($P < 0.05$, Fig. 3c, d). GLP-1 had significant effect on plasma acetaminophen at the initial time points compared with saline (timepoint 5 min, $P < 0.05$).

Plasma concentrations of insulin and C-peptide mirrored blood glucose levels (Fig. 3e–g). However, in rats receiving both secretin and GLP-1, insulin and C-peptide peaked 5 min after the oral glucose gavage at which timepoint no change in blood glucose levels was observed (Fig. 3a). When comparing $iAUC_{0-90\,min}$ of insulin and C-peptide, there was a tendency toward a lowering effect of secretin and GLP-1, but neither reached statistical significance (Secretin vs. Saline; $P_{insulin} = 0.07$ and $P_{c-peptide} = 0.09$, GLP-1 vs. Saline; $P_{insulin} = 0.09$ and $P_{c-peptide} = 0.55$ and Secretin + GLP-1 vs. Saline; $P_{insulin} = 0.69$ and $P_{c-peptide} = 0.44$) (Fig. 3f–h).

Glucose administration lowered plasma glucagon concentrations in all groups (Fig. 3i). However, secretin (either alone or in combination with GLP-1) treated rats had a significantly increased plasma concentration of glucagon during the first 5 min after administration (Secretin: 9.7 ± 1.1 vs. Saline: 6.5 ± 1.4 pmol/L, $P = 0.04$ and Secretin + GLP-1: 9.8 ± 0.7 vs. Saline: 6.5 ± 1.4 pmol/L, $P = 0.03$) but after 30 min, levels were similar to those in the control group ($P > 0.05$). Glucagon n-AUCs were lower in the group receiving GLP-1 compared with saline group ($P = 0.08$) and to the secretin-treated group ($P < 0.05$) (Fig. 3j).

Pancreatic delta cells express the Sctr and exogenous secretin increases somatostatin secretion from the perfused rat pancreas

To evaluate the potential metabolic effects of increased secretin release, we initially assessed tissue specific enrichment of the Sctr. We found that aside from the known expression of SCTRs in the duodenum, pancreatic tissue contained the Sctr transcript (Fig. 4a). However, since these values represent both expression in exocrine acinar/ductular tissue and islets, we next investigated if Sctr was present in human islets. Sctr was expressed in delta cells and detectable at lower levels in alpha and beta cells (Fig. 4b). Sctr expression were compared with Glp-1r profiles, which, expectedly, showed high expression in the beta cells and, to a lesser extent, in the delta cells (Fig. 4b). To investigate the translational relevance of rat islets to humans in regard to Sctr expression, we used an in situ hybridization approach. The Sctr was primarily found to be expressed in pancreatic delta cells and to a lesser extent in the alpha and beta cells of the rat (Fig. 4c).
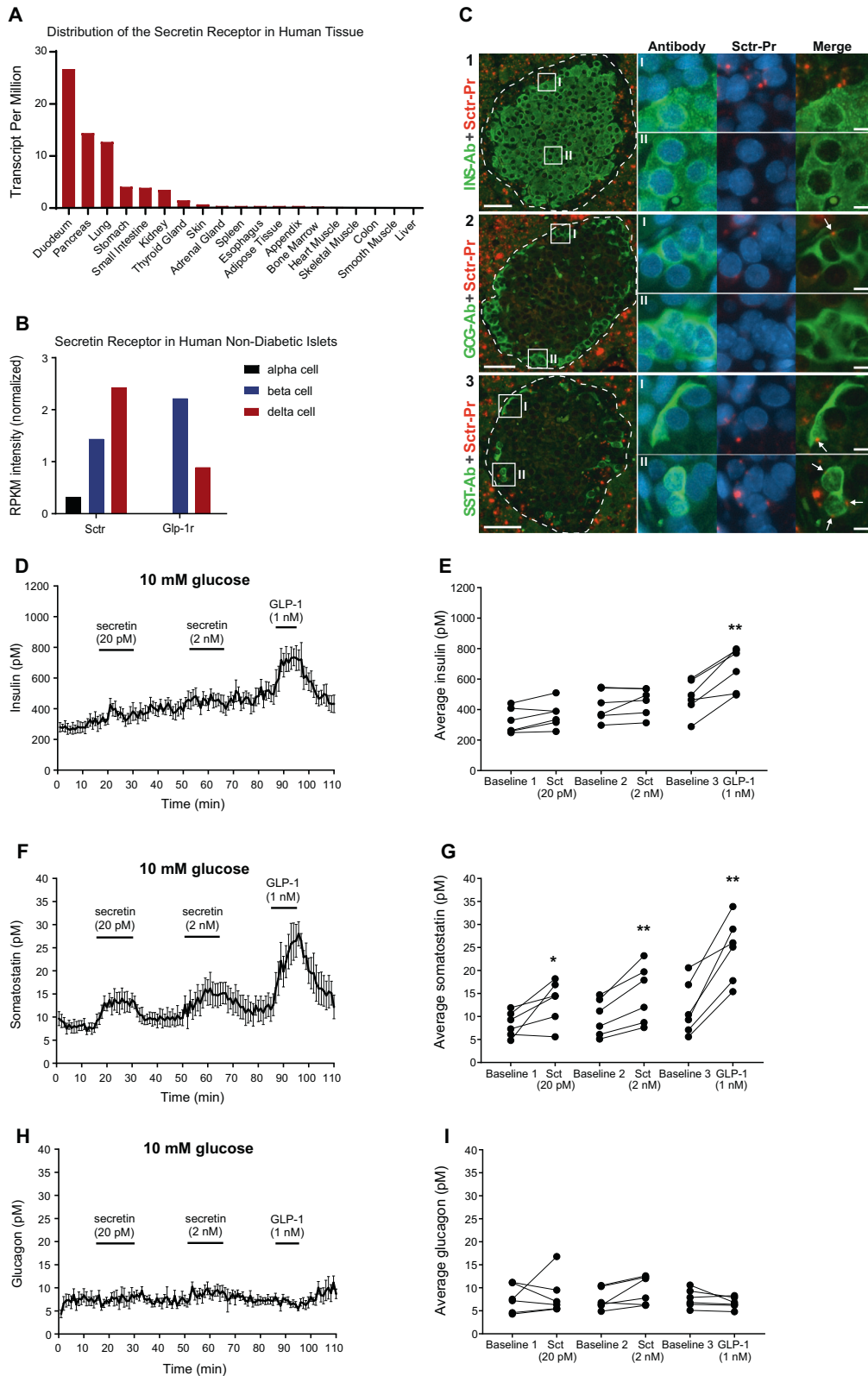
To examine whether secretin has an insulinotropic effect on the rat pancreas, we perfused the rat pancreas with 10 mmol/L glucose and administered secretin at a concentration matching post-RYGB concentrations as well as a supra-physiological concentration (20 pmol/L and 2 nmol/L, respectively) (Fig. 4d, e). GLP-1 was infused at the end of the experiment (1 nmol/L) as a positive control for insulin and somatostatin release [35–37]. Secretion of insulin continuously increased throughout the experiment independent of secretin infusion (because of the elevated glucose concentration), and the baseline secretion of insulin was therefore calculated as the average secretion before and after secretin stimulation. Insulin did not increase in response to both of the applied concentrations of secretin (Baseline: 325 ± 34 vs. Secretin (20 pmol/L): 365.9 ± 35.2 pmol/L, $P = 0.13$ and Baseline: 426.8 ± 41.7 vs. Secretin (2 nmol/L): 454 ± 36.8 pmol/L, $P = 0.56$, $n = 6$) (Fig. 4e).

Consistent with the expression of the Sctr in rat and human delta cells, secretin infusion significantly increased the secretion of somatostatin (Baseline: 8.3 ± 1.1 vs. Secretin (20 pmol/L): 13.3 ± 1.9 pmol/L, $P < 0.05$ and Baseline: 9.8 ± 1.6 vs. Secretin (2 nmol/L): 14.9 ± 2.6 pmol/L, $P < 0.05$, $n = 6$) (Fig. 4f, g).

Glucagon secretion was low, due to the high glucose concentration in the perfusion buffer, and neither secretin nor GLP-1 infusions led to significant changes in its secretion ($P > 0.18$, $n = 6$) (Fig. 4h, i).

Discussion

Here, we demonstrate that postprandial plasma concentrations of secretin are increased after RYGB surgery in obese

Secretin release after Roux-en-Y gastric bypass reveals a population of glucose-sensitive S cells in...

1867

A Distribution of the Secretin Receptor in Human Tissue

B Secretin Receptor in Human Non-Diabetic Islets

C

D 10 mM glucose

E

F 10 mM glucose

G

H 10 mM glucose

I

individuals. This may result from the anatomical rearrangement of the small intestine which diverts luminal nutrients, like glucose, to more distal sites of the small intestine, where glucose is effectively absorbed and may give rise to increased secretion of some gut hormones that are more abundant in the distal part of the small intestine [38].

◀ **Fig. 4 Expression of the secretin receptor (Sctr) and the effects of exogenous secretin on the perfused rat pancreas. a** Expression profiles of Sctr in human tissues. RNA-seq data from human tissues presented as transcripts per million (TPM) [26]. **b** Expression of Sctr and Glp-1r in human nondiabetic islets. RNA-seq data from human alpha, beta and delta cells presented as reads per kilobase million (RPKM) [23–25]. **c** Dual in situ hybridization and immunohisto-chemical staining of Sctr mRNA transcripts in rat pancreatic islets. Representative images of pancreatic islets containing in situ hybridization stained Sctr mRNA transcripts (red) and immunohistochemically stained insulin (1), glucagon (2), and somatostatin (3) (green) cells with blow-up areas. Each red dot represents a single stained mRNA transcript. Arrows indicate overlap between Sctr mRNA staining and peptide hormone staining. Dashed line outline border between pancreatic islets and exocrine pancreas. Nuclei was visualized with DAPI counterstaining (blue). Arrows indicate staining overlap. Overview scale bar, 50 μm. Blow-up scale bar, 5 μm, $n = 4$ male Wistar rats. **d–i** Effects of exogenous secretin on the perfused rat pancreas. Secretin (20 pmol/L) was infused between 16 and 30 min and secretin (2 nmol/L) was infused between 51 and 65 min. GLP-1 (1 nmol/L) was infused between 86 and 95 min as a positive control for insulin secretion **d** Insulin concentrations (pmol/L). **e** Mean concentrations of insulin at baseline (Baseline 1, 2, and 3) and following stimulation with either 20 pmol/L secretin, 2 nmol/L secretin, or 1 nmol/L GLP-1. **f** Somatostatin concentrations (pmol/L). **g** Mean concentrations of somatostatin at baseline (Baseline 1, 2, and 3) and following stimulation with either 20 pmol/L secretin, 2 nmol/L secretin, or 1 nmol/L GLP-1. **h** Glucagon concentrations (pmol/L). **i** Mean concentrations of glucagon at baseline (Baseline 1, 2, and 3) and following stimulation with either 20 pmol/L secretin, 2 nmol/L secretin, or 1 nmol/L GLP-1. Data are shown as means ± SEM. $P > 0.05$. $*P < 0.05$, $**P < 0.01$ by a one-way ANOVA with correction for multiple testing (Holm–Sidak), $n = 6$ male Wistar rats for all groups.

Increased villus length after RYGB or accelerated gastric emptying may also contribute to the observed changes in plasma secretin concentrations [39]. In addition, secretin is also produced to some extent in the biliary epithelial cells, and secretin secreted from these cells may influence total plasma secretin concentrations, although the relative importance of biliary secretin in this regard warrants further investigation. Tissue levels of secretin have been reported to be upregulated in a rodent model of RYGB [40] but post-operative plasma concentrations of secretin have to our knowledge not been reported previously.

Furthermore, we show that secretin, besides in the duo-denum, is expressed in the distal small intestine in humans and rats, and using a physiologically relevant model: the perfused rat intestine [31], we demonstrate that glucose is a strong stimulus for secretin release from the distal but not from the proximal rat small intestine. Using an inhibitor of SGLT1/2 activity (phloridzin) [34] we found that the molecular mechanism responsible for glucose-induced secretin secretion involves glucose absorption through the SGLT. SGLT-2 inhibition has gained major clinical interest due to its glucose lowering effect and reduced risk of cardiovascular disease [41]. One may therefore speculate that patients treated with nonselective SGLT inhibitors would have an altered secretin secretion profile, similar to what has

been reported for GLP-1 [42] but this remains to be explored. Previous attempts to show glucose-induced secretin secretion have been negative [7, 43–45], probably because in these studies glucose was administered to the proximal rather than the distal part of the small intestine.

Glucose-stimulated secretin release from the distal small intestine is probably not of major physiological importance in unoperated humans since glucose is mainly absorbed in the proximal part of the small intestine. However, after intake of large carbohydrate rich meals, some intraluminal glucose may reach more distal parts of the small intestine [46], and secretion under these circumstances may play a role together with GLP-1 in improving glycemic control by inhibition of gastric emptying. This putative effect is supported by our in vivo data and consistent with previous findings [2–4].

Intraluminal acidification in the distal small intestine resulted in a larger secretory secretin response compared with the proximal intestine. The physiological relevance of this finding is not clear. The acidity of the gastric chyme entering the upper part of the small intestine is rapidly neutralized by a mixture of bile, mucosal-, and pancreatic bicarbonate secretion, but the stimulatory effect of low pH in the distal small intestine on secretin-secreting cells may reflect a safety mechanism to reduce gastric emptying. The fact that also GLP-1 secretion was increased, may point to a more general effect, however, where hydrogen ions formed during digestion and perhaps fermentation in the mucosa micromilieu, stimulate ileal endocrine cells to activate the ileal brake. Further studies are required to investigate this new unexpected observation.

The observations regarding the effects of secretin on pancreatic islets are conflicting [6, 7, 47–51]. Our data support that physiological levels of secretin regulate the pancreatic secretion of somatostatin which is consistent with Sctr expression in rat and human delta cells. Although Sctr was also expressed by beta cells, secretin did not affect insulin secretion in the perfused rat pancreas whereas in vivo secretin actually led to the lowering of plasma insulin levels early after an OGTT. The underlying reason for this awaits further investigation but this may be related to prolonged gastric emptying time and to an increased secretion of somatostatin, which through paracrine effects may have overruled potential direct stimulatory effects of secretin on insulin secretion. Glucagon secretion was also not affected but this may be due to the already low levels when the pancreas was perfused in hyperglycemic conditions, thereby restricting the capability to detect further inhibition of alpha cells. However, to our surprise, there was a short-lasting increase in glucagon secretion after secretin injection in vivo, which was uninfluenced by the glucagonostatic effect of GLP-1 [52] and sympathetic stress (as this was not observed in the control group), as observed when similar doses of both peptides were injected. The underlying reason(s) is not clear.

Conclusion

Our study expands the current knowledge regarding secretin physiology and suggest that the RYGB-related increase in plasma secretin concentrations is mediated by nutrients reaching S cells located in the distal small intestine. The physiological role of glucose-sensing S cells warrant further studies but given secretin's potential effects on islet secretion and whole-body metabolism [53] it may be speculated that secretin contributes to the metabolic effects of RYGB.

Author contributions Conceived and designed research: IMM, NJWA, and JJH. Performed experiments: DBA, KVG, REK, CBC, CØ, BH, and IMM. Provided clinical samples: CM, KNBM, and SM. Provided mass-spectrometry data: PL, RK, FR, and FG. Analyzed data: IMM and NJWA. Interpreted results of experiments: IMM and NJWA. Prepared figures: IMM and NJWA. Drafted manuscript: IMM and NJWA. All authors edited and revised the manuscript and approved the final version.

Compliance with ethical standards

Conflict of interest The authors declare that they have no conflict of interest.

Publisher's note Springer Nature remains neutral with regard to jurisdictional claims in published maps and institutional affiliations.

References

1. Bayliss WM, Starling EH. The mechanism of pancreatic secretion. J Physiol. 1902;28:325–53. http://www.ncbi.nlm.nih.gov/pubmed/16992627.
2. Raybould HE, Holzer H. Secretin inhibits gastric emptying in rats via a capsaicin-sensitive vagal afferent pathway. Eur J Pharmacol. 1993;250:165–7. http://www.ncbi.nlm.nih.gov/pubmed/8119315.
3. Valenzuela JE, Defilippi C. Inhibition of gastric emptying in humans by secretin, the octapeptide of cholecystokinin, and intraduodenal fat. Gastroenterology. 1981;81:898–902. https://www.gastrojournal.org/article/S0016-5085(81)80115-1/abstract.
4. Vagne M, Andre C. The effect of secretin on gastric emptying in man. Gastroenterology. 1971;60:421–4. https://www.sciencedirect.com/science/article/abs/pii/S0016508571801221.
5. Glaser B, Shapiro B, Glowniak J, Fajans SS, Vinik AI. Effects of secretin on the normal and pathological β -cell. J Clin Endocrinol Metab. 1988;66:1138–43. https://academic.oup.com/jcem/article-lookup/doi/10.1210/jcem-66-6-1138.
6. Hisatomi A, Unger RH. Secretin inhibits glucagon in the isolated perfused dog pancreas. Diabetes. 1983;32:970–3. http://www.ncbi.nlm.nih.gov/pubmed/6137431.
7. Fahrenkrug J, Schaffalitzky de Muckadell OB, Kühl C. Effect of secretin on basal- and glucose-stimulated insulin secretion in man. Diabetologia. 1978;14:229–34. http://www.ncbi.nlm.nih.gov/pubmed/565310.
8. Dupré J, Chisholm DJ, McDonald TJ, Rabinovitch A. Effects of secretin on insulin secretion and glucose tolerance. Can J Physiol Pharmacol. 1975;53:1115–21. http://www.nrcresearchpress.com/doi/10.1139/y75-155.
9. Unger RH, Ketterer H, Dupré J, Eisentraut AM. The effects of secretin, pancreozymin, and gastrin on insulin and glucagon secretion in anesthetized dogs. J Clin Invest. 1967;46:630–45. http://www.ncbi.nlm.nih.gov/pubmed/4290022.
10. Unger RH, Ketterer H, Eisentraut A, Dupré J. Effect of secretin on insulin secretion. Lancet. 1966;288:24–6. https://www.sciencedirect.com/science/article/pii/S0140673666917491?via%3Dihub.
11. Adams TD, Davidson LE, Litwin SE, Kim J, Kolotkin RL, Nanjee MN, et al. Weight and metabolic outcomes 12 years after gastric bypass. N Engl J Med. 2017;377:1143–55. http://www.nejm.org/doi/10.1056/NEJMoa1700459.
12. Larraufie P, Roberts GP, McGavigan AK, Kay RG, Li J, Leiter A, et al. Important role of the GLP-1 axis for glucose homeostasis after bariatric surgery. Cell Rep. 2019;26:1399–.e6. http://www.ncbi.nlm.nih.gov/pubmed/30726726.
13. Holst JJ, Madsbad S. Mechanisms of surgical control of type 2 diabetes: GLP-1 is key factor. Surg Obes Relat Dis. 2016;12:1236–42. http://www.ncbi.nlm.nih.gov/pubmed/27313194.
14. Adriaenssens AE, Reimann F, Gribble FM. Distribution and stimulus secretion coupling of enteroendocrine cells along the intestinal tract. In: Comprehensive physiology. Hoboken, NJ, USA: John Wiley & Sons, Inc.; 2018. p. 1603–38. http://www.ncbi.nlm.nih.gov/pubmed/30215862.
15. Martinussen C, Bojsen-Møller KN, Dirksen C, Jacobsen SH, Jørgensen NB, Kristiansen VB, et al. Immediate enhancement of first-phase insulin secretion and unchanged glucose effectiveness in patients with type 2 diabetes after Roux-en-Y gastric bypass. Am J Physiol Endocrinol Metab. 2015;308:E535–44. http://www.physiology.org/doi/10.1152/ajpendo.00506.2014.
16. Roberts GP, Larraufie P, Richards P, Kay RG, Galvin SG, Miedzybrodzka EL, et al. Comparison of human and murine enteroendocrine cells by transcriptomic and peptidomic profiling. Diabetes. 2019;68:1062–72. http://www.ncbi.nlm.nih.gov/pubmed/30733330.
17. Brand CL, Jorgensen PN, Knigge U, Warberg J, Svendsen I, Kristensen JS, et al. Role of glucagon in maintenance of euglycemia in fed and fasted rats. Am J Physiol. 1995 ;269: E469–77.
18. Orskov C, Jeppesen J, Madsbad S, Holst JJ. Proglucagon products in plasma of noninsulin-dependent diabetics and nondiabetic controls in the fasting state and after oral glucose and intravenous arginine. J Clin Invest. 1991;87:415–23. https://doi.org/10.1172/JCI115012.
19. Orskov C, Rabenhøj L, Wettergren A, Kofod H, Holst JJ. Tissue and plasma concentrations of amidated and glycine-extended glucagon-like peptide I in humans. Diabetes. 1994;43:535–9. https://doi.org/10.2337/diab.43.4.535.

20. Baldissera FGA, Nielsen OV, Holst JJ. The intestinal mucosa preferentially releases somatostatin-28 in pigs. Regul Pept. 1985;11:251–62. https://linkinghub.elsevier.com/retrieve/pii/0167011585900576.

21. Hilsted L, Holst JJ. On the accuracy of radioimmunological determination of somatostatin in plasma. Regul Pept. 1982;4:13–31. https://linkinghub.elsevier.com/retrieve/pii/0167011582901057.

22. Wewer Albrechtsen NJ, Kuhre RE, Windeløv JA, Ørgaard A, Deacon CF, Kissow H, et al. Dynamics of glucagon secretion in mice and rats revealed using a validated sandwich ELISA for small sample volumes. Am J Physiol Metab. 2016;311:E302–9. http://www.ncbi.nlm.nih.gov/pubmed/27245336.

23. Xin Y, Kim J, Okamoto H, Ni M, Wei Y, Adler C, et al. RNA sequencing of single human islet cells reveals type 2 diabetes genes. Cell Metab. 2016;24:608–15. https://www.sciencedirect.com/science/article/pii/S155041311630434X.

24. Muraro MJ, Dharmadhikari G, Grün D, Groen N, Dielen T, Jansen E, et al. A single-cell transcriptome atlas of the human pancreas. Cell Syst. 2016;3:385–.e3. http://www.ncbi.nlm.nih.gov/pubmed/27693023.

25. Segerstolpe Å, Palasantza A, Eliasson P, Andersson E-M, Andréasson A-C, Sun X, et al. Single-cell transcriptome profiling of human pancreatic islets in health and type 2 diabetes. Cell Metab. 2016;24:593–607. https://www.sciencedirect.com/science/article/pii/S1550413116304363.

26. Uhlén M, Fagerberg L, Hallström BM, Lindskog C, Oksvold P, Mardinoglu A, et al. Tissue-based map of the human proteome. Science. 2015;347:1260419. https://science.sciencemag.org/content/347/6220/1260419.

27. Polak JM, Coulling I, Bloom S, Pearse AG. Immunofluorescent localization of secretin and enteroglucagon in human intestinal mucosa. Scand J Gastroenterol. 1971;6:739–44. http://www.ncbi.nlm.nih.gov/pubmed/4945081.

28. Van Ginneken C, Weyns A. A stereological evaluation of secretin and gastric inhibitory peptide-containing mucosal cells of the perinatal small intestine of the pig. J Anat. 2004;205:267–75. http://www.ncbi.nlm.nih.gov/pubmed/15447686.

29. Eissele R, Göke R, Willemer S, Harthus H-P, Vermeer H, Arnold R. et al. Glucagon-like peptide-1 cells in the gastrointestinal tract and pancreas of rat, pig and man. Eur J Clin Invest.1992;22:283–91. https://doi.org/10.1111/j.1365-2362.1992.tb01464.x.

30. Wewer Albrechtsen NJ, Kuhre RE, Toräng S, Holst JJ. The intestinal distribution pattern of appetite- and glucose regulatory peptides in mice, rats and pigs. BMC Res Notes. 2016;9:60. http://www.ncbi.nlm.nih.gov/pubmed/26830025.

31. Kuhre RE, Holst JJ. Mechanisms underlying gut hormone secretion using the isolated perfused rat small intestine. J Vis Exp. 2019;e58533. https://www.jove.com/video/58533/mechanisms-underlying-gut-hormone-secretion-using-isolated-perfused.

32. Kuhre RE, Christiansen CB, Saltiel MY, Wewer Albrechtsen NJ, Holst JJ. On the relationship between glucose absorption and glucose-stimulated secretion of GLP-1, neurotensin, and PYY from different intestinal segments in the rat. Physiol Rep. 2017;5. https://doi.org/10.14814/phy2.13507.

33. Gribble FM, Williams L, Simpson AK, Reimann F. A novel glucose-sensing mechanism contributing to glucagon-like peptide-1 secretion from the GLUTag cell line. Diabetes. 2003;52:1147–54. http://www.ncbi.nlm.nih.gov/pubmed/12716745.

34. Parker HE, Adriaenssens A, Rogers G, Richards P, Koepsell H, Reimann F, et al. Predominant role of active versus facilitative glucose transport for glucagon-like peptide-1 secretion. Diabetologia. 2012;55:2445–55. http://www.ncbi.nlm.nih.gov/pubmed/22638549.

35. Holst JJ. The physiology of glucagon-like peptide 1. Physiol Rev. 2007;87:1409–39. https://doi.org/10.1152/physrev.00034.2006.

36. de Heer J, Rasmussen C, Coy DH, Holst JJ. Glucagon-like peptide-1, but not glucose-dependent insulinotropic peptide, inhibits glucagon secretion via somatostatin (receptor subtype 2) in the perfused rat pancreas. Diabetologia. 2008;51:2263–70. http://www.ncbi.nlm.nih.gov/pubmed/18795252.

37. Jia X, Brown JC, Kwok YN, Pederson RA, McIntosh CHS. Gastric inhibitory polypeptide and glucagon-like peptide-1(7–36) amide exert similar effects on somatostatin secretion but opposite effects on gastrin secretion from the rat stomach. Can J Physiol Pharmacol. 1994;72:1215–9. http://www.ncbi.nlm.nih.gov/pubmed/7882187.

38. Zhang X, Young RL, Bound M, Hu S, Jones KL, Horowitz M, et al. Comparative effects of proximal and distal small intestinal glucose exposure on glycemia, incretin hormone secretion, and the incretin effect in health and type 2 diabetes. Diabetes Care. 2019;42:520–8.

39. Gehart H, van Es JH, Hamer K, Beumer J, Kretzschmar K, Dekkers JF, et al. Identification of enteroendocrine regulators by real-time single-cell differentiation mapping. Cell. 2019;176:1158–.e16. https://www.sciencedirect.com/science/article/pii/S009286741831643X?via%3Dihub.

40. Zhang C, Rigbolt K, Petersen SL, Biehl Rudkjær LC, Schwahn U, Fernandez-Cachon ML, et al. The preprohormone expression profile of enteroendocrine cells following Roux-en-Y gastric bypass in rats. Peptides. 2019. https://www.sciencedirect.com/science/article/pii/S0196978119300786?dgcid=rss_sd_all.

41. Thomas MC, Cherney DZI. The actions of SGLT2 inhibitors on metabolism, renal function and blood pressure. Diabetologia. 2018;61:2098–107. https://doi.org/10.1007/s00125-018-4669-0.

42. Osonoi T, Tamasawa A, Osonoi Y, Ofuchi K, Katoh M, Saito M. Canagliflozin increases postprandial total glucagon-like peptide 1 levels in the absence of α-glucosidase inhibitor therapy in patients with type 2 diabetes: a single-arm, non-randomized, open-label study. Diabetes Ther. 2019;1–15. https://doi.org/10.1007/s13300-019-00689-w.

43. Fahrenkrug J, Muckadell OBSde. Plasma secretin concentration in man: effect of intraduodenal glucose, fat, amino acids, ethanol, HCI, or ingestion of a meal. Eur J Clin Invest. 1977;7:201–3. https://doi.org/10.1111/j.1365-2362.1977.tb01598.x.

44. Boden G, Essa N, Owen OE, Reichle FA, Saraga W. Effects of intraduodenal administration of HCl and glucose on circulating immunoreactive secretin and insulin concentrations. J Clin Invest. 1974;53:1185–93. http://www.ncbi.nlm.nih.gov/pubmed/4815082.

45. Fahrenkrug J, Schaffalitzky De Muckadell OB, Holst JJ. Plasma secretin concentration in anaesthetized pigs after intraduodenal glucose, fat, aminoacids, or meals with various pH. Scand J Gastroenterol. 1977;12:273–9. https://doi.org/10.3109/00365527709180928.

46. Holst JJ, Gribble F, Horowitz M, Rayner CK. Roles of the gut in glucose homeostasis. Diabetes Care. 2016;39:884–92. http://www.ncbi.nlm.nih.gov/pubmed/27222546.

47. Brodows RG, Chey WY. Physiological doses of secretin do not stimulate acute insulin release. J Clin Endocrinol Metab. 1980;50:603–6. https://academic.oup.com/jcem/article-lookup/10.1210/jcem-50-3-603.

48. Ferrer RL, Medrano J, Calpena R, Diego M, Graells ML, Moltó MV, et al. Effect of exogenous cholecystokinin and secretin on pancreatic secretion of insulin and glucagon in rats: in vivo model without hepatic filter. Dig Dis Sci. 2001;46:2127–33. https://doi.org/10.1023/A:1011994327575.

49. Santeusanio F, Faloona GR, Unger RH. Suppressive effect of secretin upon pancreatic alpha cell function. J Clin Invest. 1972;51:1743–9. https://www.jci.org/articles/view/106975.

50. Jensen SL, Fahrenkrug J, Holst JJ, Kühl C, Nielsen OV, Schaffalitzky de Muckadell OB. Secretory effects of secretin on isolated perfused porcine pancreas. Am J Physiol. 1978;235:E381–6. http://www.ncbi.nlm.nih.gov/pubmed/696858.

51. Florholmen J, Vonen B, Giaever AK, Burhol PG. The effect of secretin on the glucose-induced insulin release from isolated

pancreatic islets in mice. Acta Physiol Scand. 1987;130:237–41. http://www.ncbi.nlm.nih.gov/pubmed/3300169.

52. Hare KJ, Vilsboll T, Asmar M, Deacon CF, Knop FK, Holst JJ. The glucagonostatic and insulinotropic effects of glucagon-like peptide 1 contribute equally to its glucose-lowering action. Diabetes. 2010;59:1765–70. http://www.ncbi.nlm.nih.gov/pubmed/20150286.

53. Li Y, Schnabl K, Gabler S-M, Willershäuser M, Reber J, Karlas A, et al. Secretin-activated brown fat mediates prandial thermogenesis to induce satiation. Cell. 2018;175:1561–.e12. https://www.sciencedirect.com/science/article/pii/S0092867418313242.

Affiliations

Ida M. Modvig [1,2] · Daniel B. Andersen[1,2] · Kaare V. Grunddal[1] · Rune E. Kuhre[1,2] · Christoffer Martinussen[3] · Charlotte B. Christiansen[1,2] · Cathrine Ørskov[1] · Pierre Larraufie[4] · Richard G. Kay[4] · Frank Reimann [4] · Fiona M. Gribble[4] · Bolette Hartmann[1,2] · Kirstine N. Bojsen-Møller[3] · Sten Madsbad[3] · Nicolai J. Wewer Albrechtsen[1,5,6] · Jens J. Holst [1,2]

1   Department of Biomedical Sciences, Faculty of Health and Medical Sciences, University of Copenhagen, Copenhagen, Denmark

2   Novo Nordisk Foundation Center for Basic Metabolic Research, Faculty of Health and Medical Sciences, University of Copenhagen, Copenhagen, Denmark

3   Department of Endocrinology, Hvidovre Hospital, Hvidovre, Denmark

4   Wellcome Trust-MRC Institute of Metabolic Science, University of Cambridge, Cambridge, UK

5   Department of Clinical Biochemistry, Rigshospitalet, University of Copenhagen, Copenhagen, Denmark

6   Novo Nordisk Foundation Center for Protein Research, Faculty of Health and Medical Sciences, University of Copenhagen, Copenhagen, Denmark